An Amino-Functionalized MIL-53 Metal Organic Framework with Large Separation Power for CO_2 and CH_4

Sarah Couck[1], Joeri F.M. Denayer[1,*], Gino V. Baron[1], Tom Rémy[1], Jorge Gascon[2], Freek Kapteijn[2]

[1]Department of Chemical Engineering, Vrije Universiteit Brussel, Belgium

[2] Catalysis and Engineering, Delft University of Technology, The Netherlands

Supporting Information

Contents

1. Synthesis

All chemicals were obtained from Sigma-Aldrich and were used without further purification. The synthesis of amino-MIL-53(Al) was performed as described elsewhere.[1] 2.10 mmol aluminium nitrate nonahydrate dissolved in 15 mL DMF and 3.12 mmol 2-aminoterephthalic acid dissolved in 15 ml DMF were mixed in a Teflon insert and placed in an autoclave. The autoclave was heated in an oven at 403 K for 3 days. The yellow gel product was filtered off and washed with acetone. After removal of the acetone under reduced pressure, the product was washed overnight with methanol under reflux and dried at 110°C under in vacuo for 8 h (yield ~40% yellow powder based on 2-aminoterephthalic acid).

In the case of the Amino-MIL-53 (Al) no calcination step is necessary as reported for MIL-53 (Al). Then, comparisons are made between hydrated and dehydrated structures (not between as-synthesized, low temperature and high temperature, as in the case of the bare MIL-53's: [2-4])

2. Characterization methods

The crystalline materials were analyzed by X-ray diffraction (XRD) using a Bruker-AXS D5005 with CuKα radiation. Temperature Programmed XRD (TP-XRD) was performed under dry N_2 atmosphere using temperature ramps of 1 K/min. The experimental procedure was as follows: one sample hydrated (as synthesized) was introduced in the sample cell and XRD was measured at room temperature. The sample was dehydrated under N_2 flow (100 ml/min) while gradually increasing the temperature with a ramp of 1K/min. XRD analyses were collected during the heating process and on the rehydrated sample 24 hours after cooling down. After correcting for sample displacement by using the calibrated positions of the LaB6, peak positions are accurately known within 0.01 degrees 2Theta. Scanning electron microscopy (SEM) on a Philips XL20 (15-30 kV) microscope was used to determine crystal morphology and size of the products. Elemental analyses of the solid samples were performed by Mikroanalytisches Labor Pascher (Remagen, Germany). DRIFT spectra were recorded in a Thermo Nicolet Nexus spectrometer, equipped with a liquid N_2-cooled MCT detector and a DRIFT high-temperature cell with

CaF2 windows. Spectra of pure MOF samples were collected without diluting the with KBr. The spectra were registered after accumulation of 64 scans and a resolution of 4 cm^{-1}. A flow of helium or CO_2 at 30 mL min^{-1} was maintained during the measurements. Before collecting the spectra the different samples were pre-treated under helium flow at 393 K for one hour. The spectra were recorded at room temperature. Thermogravimetric analysis was performed by means of a Mettler Toledo TGA/SDTA851e, under Air flow (100 ml (STP)/min) at a heating rates of 10 K/min.

3. Experimental adsorption techniques

a. Pulse Chromatographic experiments

Pellets of 400-500 μm, obtained by pressing the amino-MIL-53(Al) powder into a solid disc followed by crushing and sieving, were packed into a stainless steel column (1/8") with a length of 0.30 m and an internal diameter of 0.216 cm. Pulse chromatographic experiments were performed using this column to determine low coverage adsorption properties of methane, ethane, propane and CO_2. A HP-4890 gas chromatograph (GC) equipped with a thermal conductivity detector (TCD) was used. In situ activation of the adsorbent was performed under constant Helium flow by raising the temperature from ambient to 423 K at a rate of 1 K/min and maintaining this temperature overnight. Helium was used as the carrier gas. Henry adsorption constants were determined from the first moment of the response curve on the TCD after injection of a component. Adsorption enthalpy was obtained from the temperature dependence of the Henry adsorption constants using the van't Hoff equation.

b. Breakthrough experiments

Breakthrough experiments were performed using a column with a length of 30 cm and an internal diameter of 0.216 cm, packed with amino-MIL-53(Al) pellets. The experimental setup for the

breakthrough experiments allows in situ activation of the adsorbent under pure He flow. The experimental methodology is fully described in [2]. All separation experiments were performed at 303 K and total flows ranging from 10 to 70 Nml/min. The flow rates of all the pure gasses were regulated by mass flow controllers (0-100 ml/min). The gas stream at the outlet of the column was analyzed on-line with a mass spectrometer (MS). Before each experiment, the adsorbent was regenerated in situ by flowing pure He through the column and raising the temperature to 432 K at a rate of 5 K/min and keeping this temperature for 20 minutes.

c. Volumetry

Adsorption isotherms of pure CO_2 (purity of 99.995%) and CH_4 (purity of 99.95%) were determined using a volumetric device from VTI (HPA 100) using about 0.5 gram of amino-MIL-53(Al) sample. Before every measurement, the adsorbent was regenerated by raising the temperature to 423 K at a rate of 1K/min under vacuum (10^{-7} mbar). Equilibrium time varied between 5 minutes and 1 hour.

4. Characterization

No crystals suitable for single crystal X-ray structure determination could be obtained. The broadness of the peaks in the XRD spectrum is related with to the small particle size of this sample. Attempts to measure particle size distribution by means of laser diffraction were not successful due to the small particle size. Hence, the particles must be smaller than 200 nm (the maximum resolution of the used laser diffraction setup).In a previous study, larger crystals of this material were grown using the same synthesis method. For that sample, a much more defined XRD pattern was obtained. In order to determine the structure, the one reported for the Amino- MIL-53 (Fe) reported by Buaer *et.al.* was used as starting point. After substituting Fe by Al, the structure was optimized [5]. The excellent agreement of the experimental XRD with the simulated structure demonstrates the formation of the amino-MIL-53(Al) phase (Figure S1). The crystallographic data are summarized in Table S1. For MIL-53, different

open and closed structures have been reported in literature [2]. Although a direct comparison between the present structure and the MIL-53 structures reported by Loiseau et al [2] should be done with precaution since the activation method for the amino-MIL-53 sample is different to the one reported by Loiseau et al. for MIL-53, the present structure closely resembles the "as synthesized (as)" and the "high temperature (ht)" forms, but not the "low temperature (lt)" structure.

Results from elemental analysis are as follows for the dried material (% wt.): C: 48.6, H: 3.5, O: 33.9, N: 4.5, Al: 8.25. The obtained N/Al ratio in the MOF (0.54) fits well the expected one (0.52).

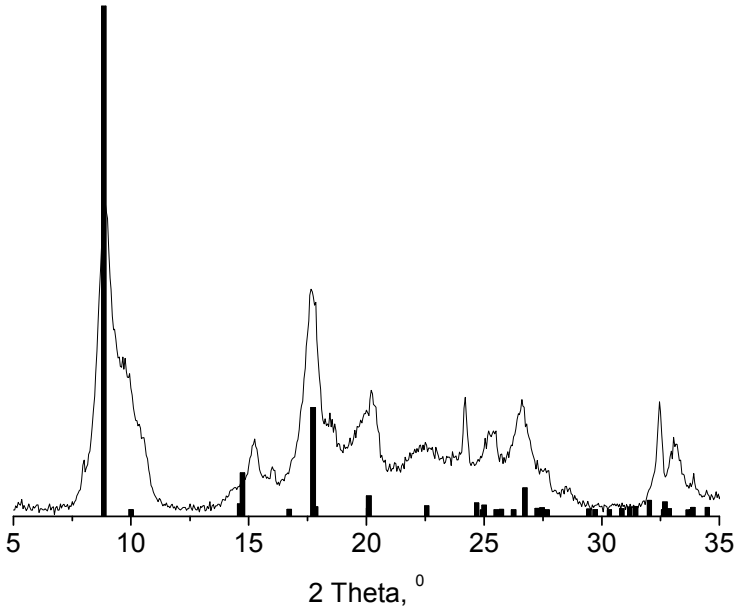

Figure S1: Experimental XRD data vs. simulated Amino MIL-53(Al) structure.

Table S1

Phase data

Space-group	I m m a (74) - orthorhombic
Cell	a=6.9177(14) Å b=17.668(3) Å c=12.120(3) Å a/b=0.3915 b/c=1.4578 c/a=1.7520 V=1481.33(54) Å^3 Z=4

Atomic parameters

Atom	Ox.	Wyck.	Site	S.O.F.	x/a	y/b	z/c	U [Å^2]
Al		4c	.2/m.		1/4	1/4	1/4	
O1		4e	mm2		0	1/4	0.17495(8)	
H1		4e	mm2		0	1/4	0.1093(7)	0.125(13)
O2		16j	1		0.33831(7)	0.16825(3)	0.14675(5)	
C1		8h	m..		1/2	0.14008(6)	0.12281(10)	
C2		8h	m..		1/2	0.06758(7)	0.05927(11)	
C3		16j	1		0.32914(14)	0.03378(5)	0.02998(10)	
H3		16j	1	0.75	0.20750	0.05550	0.05100	0.0820
N1		16j	1	0.25	0.1479(5)	0.0525(2)	0.0730(5)	
H1A		16j	1	0.25	0.13760	0.08850	0.12290	0.2550
H1B		16j	1	0.25	0.04410	0.02830	0.05030	0.2550

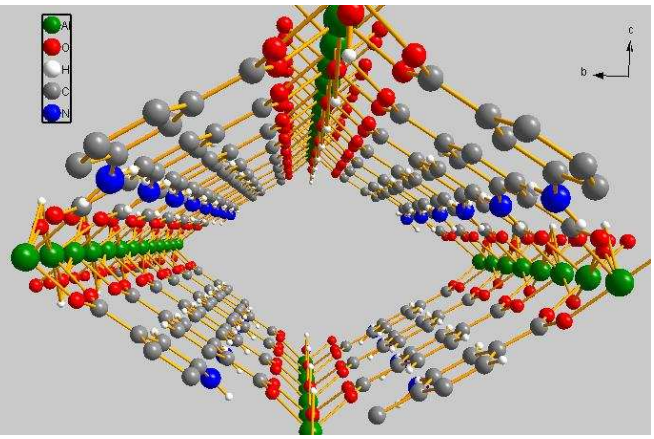

Figure S2. Amino MIL-53 (Al). Left: View along the a axis of the amino functionalized 1D channels (red: oxygen; light grey: carbon atoms; dark grey: Al atoms and blue: nitrogen atoms). Structure was obtained after Rietveld refinement of the XRD pattern.

The DRIFT spectrum corresponding to the amino-MIL-53(Al) is shown in Figure S3. For comparison, the IR spectrum for the MIL-53 as reported in reference [2] is shown. Several differences can be appreciated when comparing the amino-functionalized sample with the non functionalized MIL-53: two new clear bands appear at 3370 and 3490 cm^{-1} and a new broad band in the range 3500-2500 cm^{-1} appears in Amino MIL-53 (Al). Bands at 3370 and 3490 cm^{-1} correspond with the symmetric and asymmetric stretching of primary amines, which demonstrates the presence of amino groups, moreover, the main absorption in the 3500-2500 range is due to hydroxyl groups perturbed by the NH_2 groups and forming hydrogen bonds of medium strengths [6]. The hydroxyl groups of the trans corner sharing octahedra $AlO_4(OH)_2$ chains give rise to only one ν(OH) band at 3700 cm^{-1} with a shoulder near 3660 cm^{-1}, in contrast with the 2 ν(OH) bands reported for the non functionalized MIL-53 (Al) but in agreement with the spectrum reported for MIL-53 (Cr) [4] (shifted 50 cm^{-1} to lower wavenumbers).

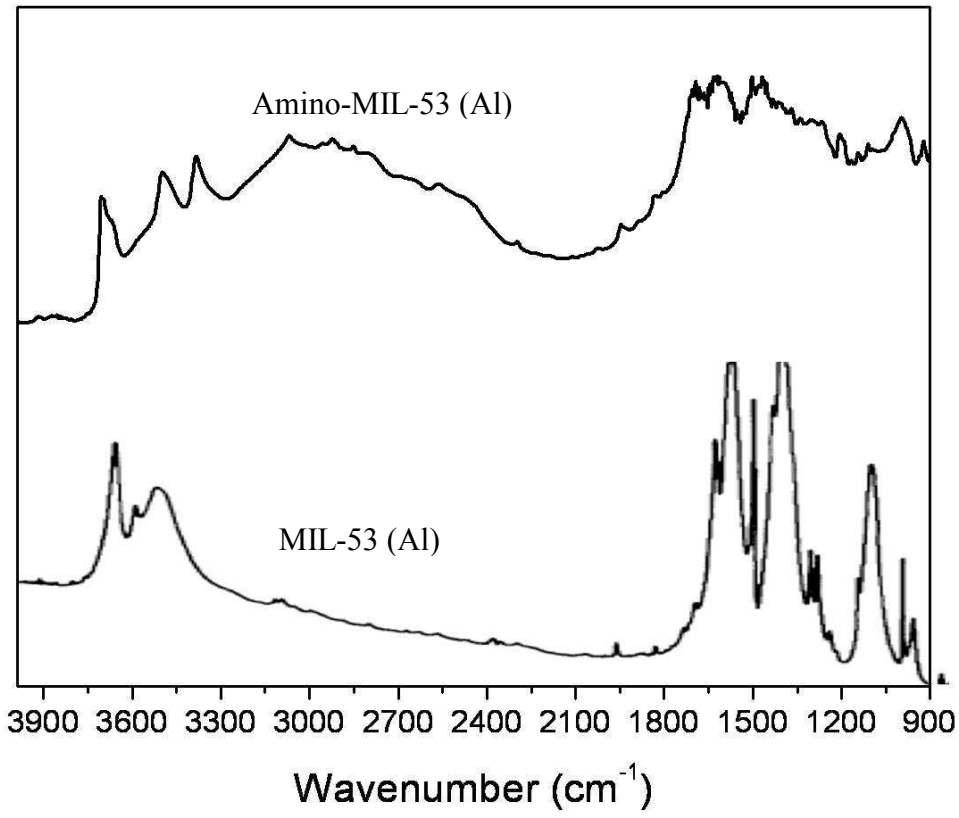

Figure S3: DRIFTS spectrum of the activated Amino-MIL-53 (Al) (top) vs IR spectrum (transmittance) of MIL-53 (Al) (down, as reported in reference [2]).

Adsorption of CO_2 was followed by in situ DRIFTS under continuous CO_2 flow in order to identify the different interactions with the framework. The corresponding spectra obtained after substracting the MOF background are shown in figure S4. Four bands at 669, 661, 655 and 649 cm^{-1} are observed. Two bands (655 and 669 cm^{-1}) correspond with the CO_2 adsorption as observed in IRMOF-3 [1] and the other two bands (661 and 649 cm^{-1}) correspond with previous observations for MIL-53 [4], without amino groups. This strongly suggests the adsorption of CO_2 in two different ways, forming Electron-Donor-Acceptor (EDA) complexes with both -NH_2 and -OH groups of the structure.

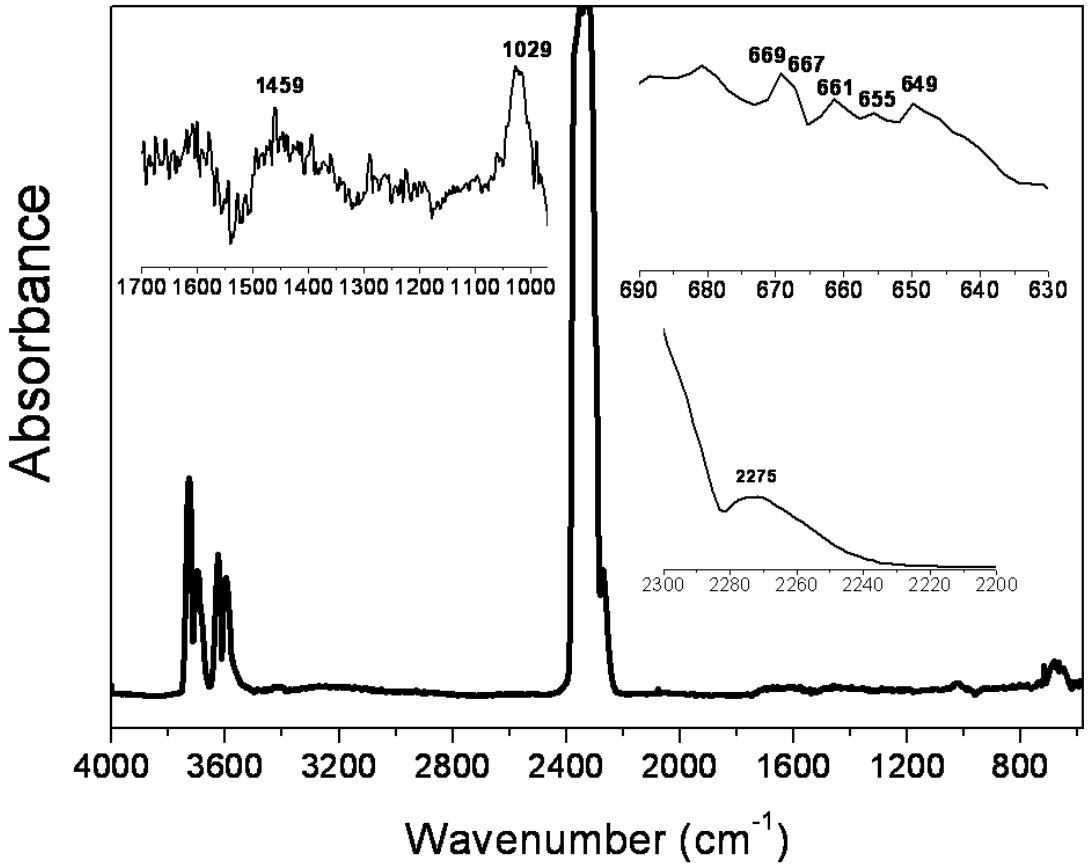

Figure S4.DRIFTs spectra of activated Amino-MIL-53(Al) after introduction of CO_2 into the cell at room temperature.

On the low wave-numbers side of the ν_3 frequency we observe a new band not related with the gas phase (2275 cm^{-1}). The high and low ν_2 frequency bands of CO_2, assigned to the out-of plane and in-plane bending modes, respectively, should lead to a lower ν_3 frequency than that observed in the gas

phase (2349 cm^{-1}), which is also expected in the case of EDA complexes involving CO_2 as an electron acceptor [7].

In addition, several new peaks can be observed in the range 1000–1700 cm^{-1}. Amines may react with CO_2 to form carbamate species. Amonium carbamate species usually yield large number of low-intensity bands in the range 1400-1700 cm^{-1} [8]. The latter are in equilibrium with the carbamic acid species (DRIFT band around 1450 cm^{-1}). Carbamate species can react with adsorbed water or surface hydroxyl groups forming carbonates, bicarbonates or formates. In fact, the broad band appearing at 1029 cm^{-1} in the Amino MIL-53 (Al) may be related to the formation of hydrogen carbonates (ν_{CO3} vibration) [9] due to the interaction of CO_2 with the hydroxyl groups of the MOF.

Figure S5 shows the temperature programmed XRD analysis in N_2 flow of the Amino-MIL-53(Al) sample starting form a hydrated sample at room temperature. As in the case of MIL-53, it seems that the dehydration-hydration process is fully reversible, indicating a very large breathing effect that involves a displacement of the chains during hydration without any change of the topology. This effect is probably due to the creation of strong hydrogen bonds between the water molecule and the hydrophilic parts of the pore: oxygen atoms, OH and NH_2 groups. Moreover, the presence of amino groups on the benzyl linkers seems to increase the breathing effect when compared with the same structure without such functionality.

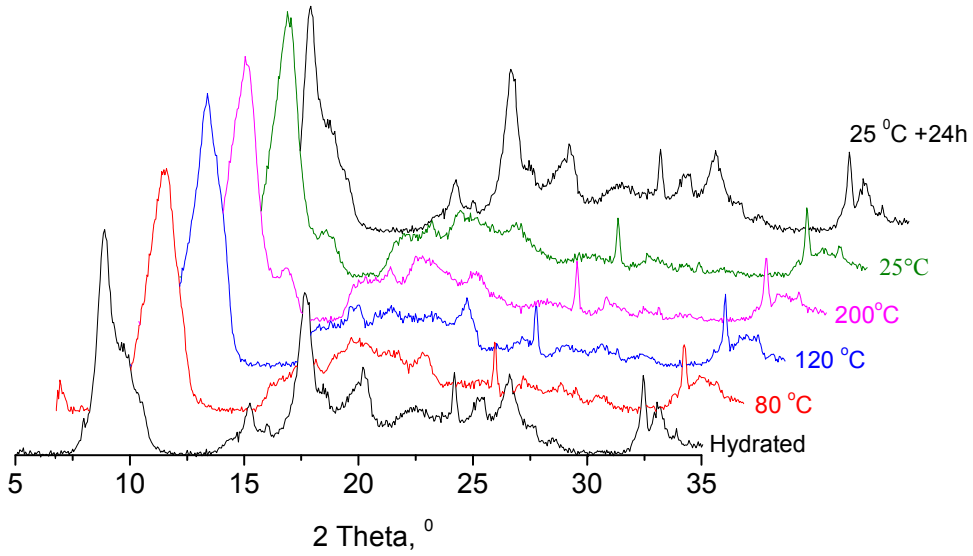

Figure S5: TPXRD analysis of the Amino-MIL-53 (Al).

The TGA profile obtained on the activated material, after contacting to the atmosphere, is shown in Fig. S6. Only a small amount of water is desorbed below 100°C, no solvent molecules were present in the activated sample.

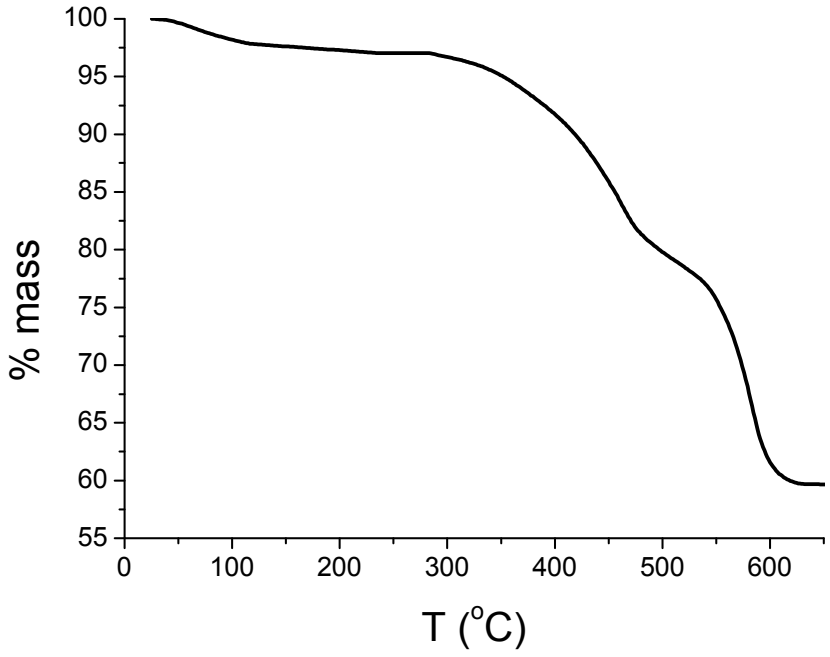

Figure S6: TGA analysis of the Amino-MIL-53 (Al).

5. Results of pulse chromatography

Figures S7 and S8 show the van 't Hoff plots of CO_2, ethane and propane on amino-MIL-53(Al) and MIL-53(Al). Adsorption enthalpies are summarized in Table S2 and S3.

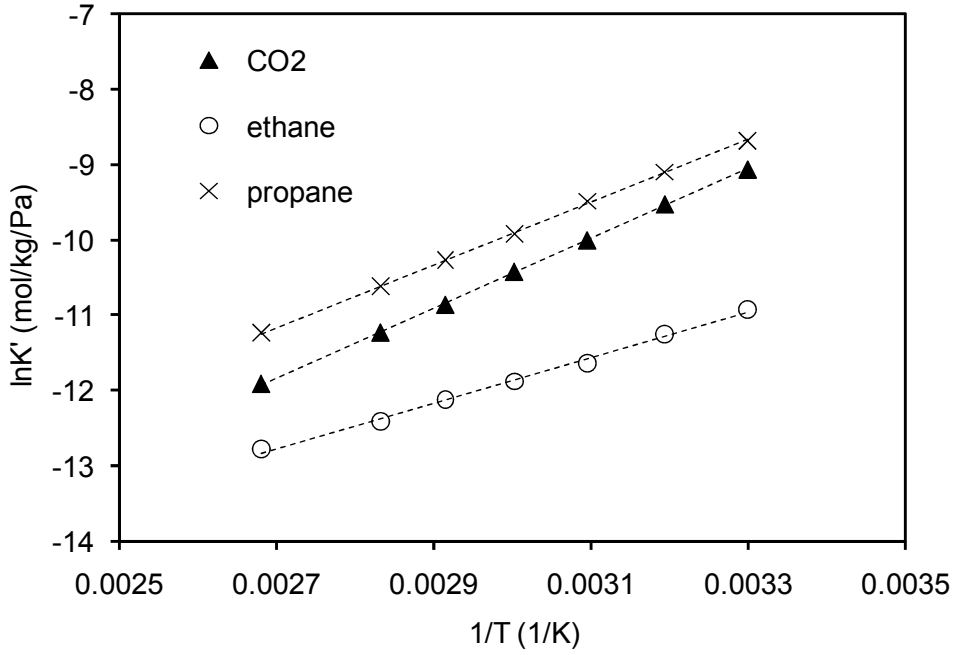

Figure S7: Van't Hoff plots of CO_2, ethane and propane on amino-MIL-53(Al)

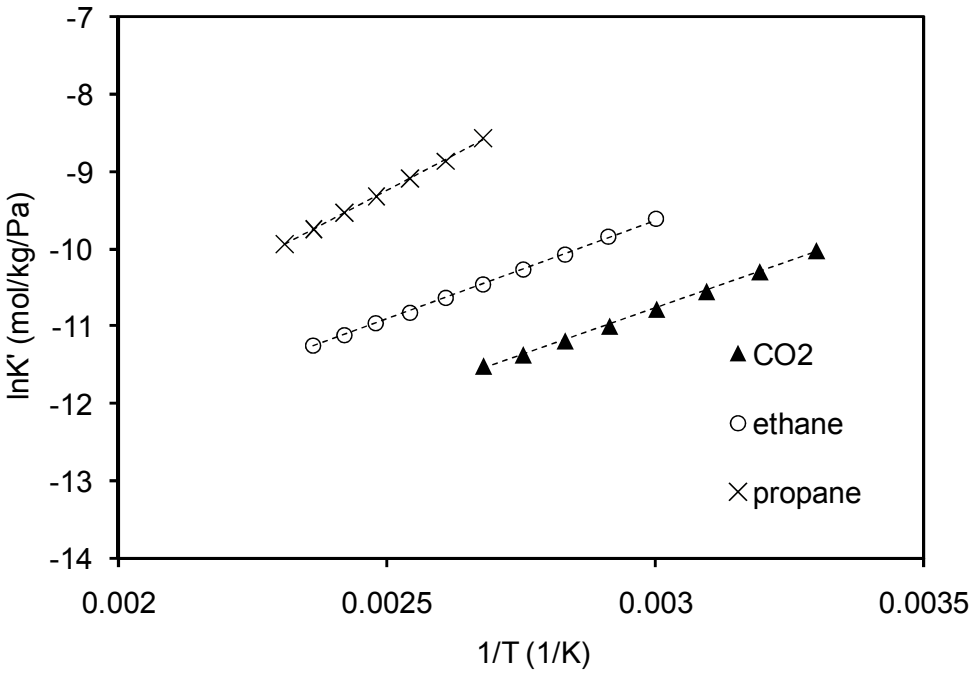

Figure S8: Van't Hoff plots of CO_2, ethane and propane on MIL-53(Al)

Table S2. Low coverage adsorption properties on amino-MIL-53(Al)

	Retention time (30°C) (min.)	K' (30°C) (mol/kg/Pa)	$-\Delta H_0$ (kJ/mol)
CO_2	5.65	$1.16\ 10^{-4}$	38.4
CH_4	< 0.1	$< 1.4\ 10^{-6}$	< 20[a]
C_2H_6	0.91	$1.81\ 10^{-5}$	25.1
C_3H_8	8.37	$1.72\ 10^{-4}$	34.7

[a] extrapolated from ethane, propane and butane data

Table S3: Zero coverage adsorption enthalpy of ethane, propane and CO_2 on amino-MIL-53(Al) and MIL-53(Al)

	$-\Delta H_0$ (kJ/mol)	
	MIL-53(Al)	amino-MIL-53(Al)
CO_2	20.1	38.4
CH_4	-	< 20[a]
C_2H_6	21.2	25.1
C_3H_8	30.4	34.7

[a] extrapolated from ethane, propane and butane data

References:

[1] J. Gascon, U. Aktay, M.D. Hernandez-Alonso, G.P.M. van Klink, and F. Kapteijn, J. Catal. 261 (2009) 75-87.

[2] T. Loiseau, C. Serre, C. Huguenard, G. Fink, F. Taulelle, M. Henry, T. Bataille, and G. Ferey, Chemistry-a European Journal 10 (2004) 1373-1382.

[3] C. Serre, F. Millange, C. Thouvenot, M. Nogues, G. Marsolier, D. Louer, and G. Ferey, J. Am. Chem. Soc. 124 (2002) 13519-13526.

[4] A. Vimont, A. Travert, P. Bazin, J.C. Lavalley, M. Daturi, C. Serre, G. Ferey, S. Bourrelly, and P.L. Llewellyn, Chem. Commun. (2007) 3291-3293.

[5] S. Bauer, C. Serre, T. Devic, P. Horcajada, J. Marrot, G. Ferey, and N. Stock, Inorg. Chem. 47 (2008) 7568-7576.

[6] L. Regli, S. Bordiga, C. Busco, C. Prestipino, P. Ugliengo, A. Zecchina, and C. Lamberti, J. Am. Chem. Soc. 129 (2007) 12131-12140.

[7] S.G. Kazarian, M.F. Vincent, F.V. Bright, C.L. Liotta, and C.A. Eckert, J. Am. Chem. Soc. 118 (1996) 1729-1736.

[8] R. Srivastava, D. Srinivas, and P. Ratnasamy, Microporous Mesoporous Mater. 90 (2006) 314-326.
[9] C. Binet, M. Daturi, and J.-C. Lavalley, Catal. Today 50 (1999) 207-225.